Effects of screened electron-phonon interactions in quantum-well wires

1993 J. Phys.: Condens. Matter 5 2203

(http://iopscience.iop.org/0953-8984/5/14/017)

J. Phys.: Condens. Matter 5 (1993) 2203–2212. Printed in the UK

Effects of screened electron–phonon interactions in quantum-well wires

B Tanatar
Department of Physics, Bilkent University, Bilkent, 06533 Ankara, Turkey

Received 23 November 1992

Abstract. We study the effects of dielectric screening on scattering rates due to electron–phonon interactions in quasi-one-dimensional quantum-well wires. We consider the interaction of confined electrons with bulk polar-optical and acoustic phonons. Acoustic phonons are examined, both in the deformation potential and the piezoelectric couplings. Screening effects are included via a temperature-dependent dielectric function $\epsilon_T(q)$ in the random-phase approximation, by renormalizing the electron–phonon interaction. Numerical results are given for the GaAs system in the quantum-size limit where a lowering of screened electron–phonon scattering rates is found. The effects of screening are most significant for the electron–optical-phonon interaction.

1. Introduction

New developments in molecular beam epitaxy technology have made possible the fabrication of electronic structures based on the confinement of electrons in an essentially one-dimensional (1D) semiconductor. In these synthetic materials, the electron gas is quantized in two transverse directions, so the charge carriers can only move in the longitudinal direction. Since the electron gas has a small but finite extent in the confined directions compared with the axis of free motion, such structures are also named quasi-one-dimensional (Q1D) systems. Owing to the limited number of available final states during the scattering process, the mobility of such systems is considerably enhanced, making them potentially important for high-speed device applications. Since their early prediction [1] and subsequent fabrication [2–6], there has been a lot of interest in the transport properties of Q1D systems. Scattering mechanisms due to various processes have been examined both theoretically and experimentally [7–13]. A transport theory in 1D or Q1D semiconductor structures has been developed for scattering mechanisms such as impurity [14], acoustic-phonon [7, 15], and optical-phonon [8, 9, 15] interactions. A recent review that discusses many properties of 1D semiconductor systems has also appeared [16].

The effects of electron–acoustic-phonon scattering in quantum-well wires were first considered by Arora [7]. Riddock and Ridley [9] and Leburton [10] studied the electron–optical-phonon interaction in an infinite quantum-well model, finding that the 1D emission rates are less than the corresponding 3D rates. The size dependence of scattering rates in these 1D semiconductor materials were also reported by Leburton [10]. Constantinou and Ridley [17] considered a finite quantum-well and calculated the electron–polar-optical-phonon scattering rates within the effective-mass

0953-8984/93/142203+10$07.50

approximation for a Q1D cylindrical quantum-well wire. They found that the scattering rates were lowered compared to the infinite confining-potential approximation.

Another line of attack on the electron–phonon scattering rates for quantum-well wires has been through Monte Carlo simulations [10, 18, 19]. In these calculations, optical- and acoustic-phonon scattering in Q1D systems with many subbands are studied for the size and confining potential-well height dependence. Many-body calculations for self-consistent polaron scattering rates [12] and polaronic energy [20] in Q1D structures have also been reported.

The scattering rates and mobilities for rectangular Q1D systems due to piezoelectric phonons have also been studied [21,22]. The general conclusion of such investigations is that the piezoelectric scattering-limited mobilities in GaAs, InSb, and InAs are smaller than the acoustic-phonon (deformation potential coupling) limited mobility, except for strongly piezoelectric materials such as CdS and ZnO, where piezoelectric scattering is dominant.

Mobility measurements and calculations in semiconductor structures have always been very important in determining the various scattering mechanisms within such systems. A detailed and comparative study on phonon-limited mobility in Q1D semiconductors was given by Fishman [15], in which a simple model for the envelope wavefunction is employed.

We note that the transport relaxation time, τ_t, and the single-particle lifetime, τ_s, are in general different quantities. The relaxation time τ_t is what enters the mobility calculations, whereas the single-particle lifetime or the scattering time is related to the self-energy ($\tau_s^{-1} \sim \operatorname{Im}\Sigma(k, \epsilon_k)$). Only when the scattering potential is a δ function do we have $\tau_t = \tau_s$, and both transport and single-particle properties are characterized by the same quantity.

Screening effects have long been recognized as reducing the effects of the electron–phonon interaction in semiconductor structures in various dimensions. In the usual treatment of scattering or relaxation-time calculations, these screening effects have been incorporated by considering the Thomas–Fermi or Debye screening lengths in the appropriate electron–phonon interaction. We notice that for the Thomas–Fermi screening approach to be valid, the wavevectors of interest must satisfy $k \ll k_F$, where k_F is the Fermi wavevector. In the case of the electron–optical-phonon interaction, wavevectors such that $k \sim k_0$ are relevant, where $k_0 = (2m\omega_0/\hbar^2)^{1/2}$ and ω_0 is the optical-phonon frequency. Consequently, the Thomas–Fermi static screening of the electron–phonon interaction is expected to be applicable if $k_0 \ll k_F$. For GaAs heterostructures this implies the condition $n > 10^{18}\,\mathrm{cm}^{-3}$ on the electron density (which corresponds to $n \sim 10^6\,\mathrm{cm}^{-1}$ for 1D semiconductors). This is much higher than the electron densities typically encountered in experiment [2]. Better approximations to screening, namely taking the full wavevector dependence of the dielectric function $\epsilon(q)$ into account, are rarely used. Thus, motivated by the work of Constantinou and Ridley [17], we investigate the possible reduction in the scattering rates of Q1D quantum-well wires due to the effects of screened electron–phonon interactions.

In this paper, our aim is to study the scattering rates due to electron–phonon interactions in Q1D structures. More specifically, we examine the electron–optical-phonon and electron–acoustic-phonon interactions. Acoustic phonons are considered both in the deformation potential and the piezoelectric couplings. We then investigate the effects of screened electron–phonon interactions on these phonon-limited scattering rates. Screening is introduced through the dielectric function $\epsilon(q)$ for which we employ the random-phase approximation (RPA). The dielectric

response function for a Q1D semiconducting system has been calculated by Lee and Spector [23]. Screening effects via a temperature-dependent 1D dielectric function $\varepsilon_T(q)$ on the phonon-limited mobility were considered by Fishman [15]. We also note that electronic properties of the Q1D structures arising from electron-impurity and electron-electron interactions will not be discussed here.

The rest of this paper is organized as follows. In the next section we introduce the wavefunction and energy levels for electrons confined in a cylindrical quantum wire, derive expressions for scattering rates due to various electron–phonon interactions, and introduce the temperature-dependent dielectric function $\varepsilon_T(q)$. In section 3 we present our numerical results on the phonon emission and absorption rates for electron–optical-phonon scattering, electron–acoustic-phonon interaction with deformation potential coupling, and electron–acoustic-phonon interaction with piezoelectric coupling. Finally, we conclude with a brief summary.

2. Theory

We consider a model of an electron gas, quantized in two transverse directions, so that the charge carriers can only move in the longitudinal direction. We choose the cross section of the system to be circular with radius R, so the quantum wire geometry becomes cylindrical. In the quantum-size limit (QSL), the radius R of the quantum-well wire is much smaller than the thermal de Broglie wavelength of the charge carriers, so that only the ground state (lowest) subband is populated. In the model of an infinite potential well confining the charge carriers, the normalized effective-mass wavefunction is given by

$$\psi(\rho,\phi,z) = \begin{cases} J_n(k_{n,l}\rho)\,\mathrm{e}^{\mathrm{i}n\phi}\,\mathrm{e}^{\mathrm{i}k_z z}/[(\pi R^2)^{1/2}\,J_{n+1}(k_{n,l}R)] & \rho \leqslant R \\ 0 & \rho > R \end{cases} \tag{1}$$

with the corresponding energy

$$E = \frac{\hbar^2}{2m}(k_z^2 + k_{n,l}^2)\,. \tag{2}$$

Here $k_{n,l} = x_{n,l}/R$ where $x_{n,l}$ is the lth root of the Bessel function $J_n(x)$.

The single-particle scattering rates (we use the notation $\tau = \tau_s$ hereafter to denote the single-particle scattering time mentioned in the previous section) can be obtained from

$$\frac{1}{\tau^{\{\substack{e\\a}\}}(k_z)} = \sum_{k_z'} W^{\{\substack{e\\a}\}}(k_z,k_z') \tag{3}$$

where the transition probability $W^{\{\substack{e\\a}\}}(k_z,k_z')$ of an electron from a state k_z to k_z' by emitting or absorbing a phonon is given by the Fermi Golden Rule

$$W^{\{\substack{e\\a}\}}(k_z,k_z') = \frac{2\pi}{\hbar}\left|M^{\{\substack{e\\a}\}}\right|^2 \delta\big(E(k_z') - E(k_z) \pm \hbar\omega_q\big). \tag{4}$$

The electron–phonon matrix element corresponding to the annihilation and creation of one phonon (upper and lower signs, respectively) is

$$M^{\{\substack{e\\a}\}} = \langle k_z', N_q \pm 1|H_{e-ph}|k_z, N_q\rangle \tag{5}$$

where N_q is the phonon occupation factor and the electron–phonon interaction can be written as

$$H_{e-ph} = \sum_q C(q)(b_q e^{iq\cdot r} + b_q^\dagger e^{-iq\cdot r}) \tag{6}$$

in which $b_q^\dagger$ and b_q are the phonon creation and annihilation operators, respectively. For polar optical phonons the interaction strength is

$$|C(q)|^2 = 2\pi e^2 \hbar\omega_0 \left(\frac{1}{\epsilon_\infty} - \frac{1}{\epsilon_0}\right) \frac{1}{q^2} \tag{7}$$

whereas for acoustic phonons coupled through a deformation potential we have

$$|C(q)|^2 = \frac{\hbar D^2}{2dv_s} q \tag{8}$$

and for acoustic phonons in the piezoelectric coupling

$$|C(q)|^2 = \frac{\hbar K^2 e^2 v_s}{2\epsilon_0} \frac{1}{q}. \tag{9}$$

In the above expressions for $C(q)$, ϵ_∞ and ϵ_0 are the high-frequency and static dielectric constants of the medium, D and K are the deformation potential and piezoelectric constants, v_s is the sound velocity and d is the mass density.

Expressing the interaction Hamiltonian (6) in cylindrical coordinates is facilitated by the following expression:

$$e^{\pm iq\cdot r} = e^{\pm q_z z}\left(J_0(q_\perp \rho) + 2\sum_{n=1}^{\infty}(\pm i)^n J_n(q_\perp \rho)\cos(n\phi)\right) \tag{10}$$

where we have used the following notation: $q = (q_\perp, q_z)$ and $r = (\rho, \phi, z)$. In this work, we consider only the lowest subband, thus the term involving summation over the index n in (10) does not contribute to the scattering rate. In systems where higher subbands are also occupied, the above expression can be conveniently employed.

The effects of screening have been included by renormalizing the electron–phonon interaction by the dielectric function, namely $H_{e-ph} \rightarrow H_{e-ph}/\varepsilon(q)$. Here the dielectric function is three-dimensional, since we consider the interaction of electrons with bulk phonons. Note also that the wavevector summation in (6) is over the 3D q values. In the approximations where a sum over q is not needed, the 1D expression for the dielectric function $\varepsilon(q)$ has been used [15]. We use the random-phase approximation (RPA) for the static dielectric function, which is given at zero-temperature by

$$\varepsilon(q) = 1 + \frac{2\alpha r_s}{\pi x^2}\left(1 - \frac{(1-x^2/4)}{x}\ln\left|\frac{1-x/2}{1+x/2}\right|\right) \tag{11}$$

where $\alpha = (4/9\pi)^{1/3}$, $r_s = a/a_B$ is the electron gas parameter, and $x = q/2k_F$. The temperature-dependent dielectric function can be obtained by simply integrating

over the frequency-dependent dielectric function at zero temperature. We quote the final result for the temperature-dependent static dielectric function [24]:

$$\varepsilon_T(q) = 1 + \frac{\alpha r_s}{2\pi} \frac{1}{(k/2k_F)^3} g(k) \tag{12}$$

where

$$g(k) = \int_0^\infty \frac{y\,dy}{\exp[E_F(y^2 - \mu/E_F)/k_B T] + 1} \ln\left|\frac{k/2k_F + y}{k/2k_F - y}\right| \tag{13}$$

in which E_F is the Fermi energy at $T = 0$, μ is the chemical potential to be determined implicitly from the finite temperature distribution function, and k_B is the Boltzmann constant. The dielectric function thus obtained does not make use of the wavefunctions of (1), therefore the geometric confinement of electrons are neglected at this level of approximation.

3. Results and discussion

We have used material parameters appropriate for GaAs to perform numerical calculations. The electron–acoustic-phonon interaction considered here within the deformation potential model is characterized by the deformation potential $D = 13.5\,eV$, a mass density of the system of $d = 5.3\,g\,cm^{-3}$, and the longitudinal sound velocity in GaAs $v_s = 5.37 \times 10^5\,cm\,s^{-1}$. For acoustic phonons in the piezoelectric coupling the dimensionless piezoelectric constant is given as $K = 0.052$. The acoustic phonon energies here are taken to be $\hbar\omega_q = \hbar v_s q$. In the case of the electron–optical-phonon interaction, we assume the phonons are dispersionless and have energy in the bulk $\hbar\omega_0 = 36.2\,meV$. The values of the high-frequency ϵ_∞ and static ϵ_0 dielectric constants are taken to be 10.9 and 12.9, respectively, and we have used the band mass of electrons, $m = 0.067m_e$, where m_e is the bare electron mass. We take the electron density of the GaAs to be $n = 1.3 \times 10^{17}\,cm^{-3}$, which corresponds to $E_F \approx 14\,meV$ (around zero temperature), and $k_F = 0.016\,Å^{-1}$. These numbers indicate that only the $n = 0$ level will be populated for $R \leqslant 150\,Å$, making our quantum-size limit assumption valid (see also [13] for similar considerations). Also, the thermal de Broglie wavelength λ_T at $T = 300\,K$ is around 300 Å.

We first show our results for the electron–optical-phonon interaction. In figure 1 the inverse scattering time τ^{-1} is depicted for two different wire radii, (*a*) $R = 50\,Å$ and (*b*) $R = 100\,Å$, as a function of the initial electron energy E in the z direction. The full curves indicate the effects of the screened electron–phonon interaction on τ^{-1}, whereas the broken curves are obtained without screening. The upper and lower curves show emission and absorption rates, respectively. We observe that the screening effects lower the scattering rates in general, and in the case of the $R = 50\,Å$ wire this reduction is about 70%. As the wire radius increases, screening effects seem slightly to increase. For instance, the reduction in the emission and absorption rates becomes about 75% for $R = 100\,Å$. Constantinou and Ridley [17] have also found a reduction in the scattering rates (by about 25%) due to the inclusion of a finite well height for $R = 50\,Å$. Note also the scales in figures 1(*a*) and (*b*), to see the change in the scattering rate τ^{-1} as the wire radius R varies.

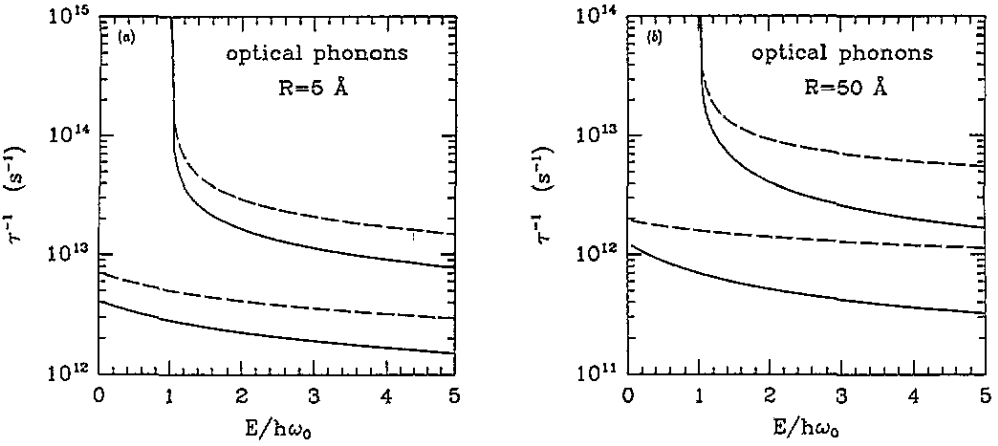

Figure 1. The inverse scattering time τ^{-1} due to the electron–optical-phonon interaction for the size quantum limit in a quantum-well wire of circular cross-section, (a) with radius $R = 50$ Å and (b) with radius $R = 100$ Å. Full and broken curves give τ^{-1} with and without screening, respectively, for emission (top curves) and absorption (bottom curves) processes at $T = 300$ K.

In figure 2 we present our results for the scattering rates due to the electron–acoustic-phonon interaction in the deformation potential coupling. The size dependence of τ^{-1} (a) $R = 50$ Å and (b) $R = 100$ Å, is plotted as a function of the initial energy E, and we again use the polar-optical phonon energy $\hbar\omega_0$ for scaling purposes. The full and broken curves indicate the scattering rates with and without dielectric screening, respectively. In contrast to the calculation for electron–optical-phonon scattering, here we resort to the elastic approximation, namely $E(k_z)$ or $E(k_z') \gg \hbar\omega_q$, and replace the energy conservation expression $\delta\big(E(k_z) - E(k_z') \pm \hbar\omega_q\big)$ by $\delta\big(E(k_z) - E(k_z')\big)$. We observe that the screening effects in the case of the electron–acoustic-phonon interaction in deformation potential coupling are not so pronounced as compared to the electron–optical-phonon scattering. In fact, for the $R \approx 50$ Å radius wire we see a 20% reduction in the calculated scattering rate.

In figures 3(a) and (b), we show the scattering rates due to the electron–acoustic-phonon interaction in the piezoelectric coupling. As in figure 2, we use $\hbar\omega_0$ for scaling purposes. The full and broken curves give the scattering rates with and without dielectric screening, respectively. As in the previous cases, the effects of the screened electron–phonon interaction increases as the wire radius increases. Both for the deformation potential and piezoelectric coupled acoustic phonons we have only reported the emission rates, since at the temperature of interest here (300 K) the phonon occupation factors N_q and $N_q + 1$ do not differ much, and the equipartition approximation is valid.

The scattering rate results we have presented here were at $T = 300$ K. The relative importance of various electron–phonon interactions at this temperature may be assessed by the scales of figures 1(a)–3(b). It has long been known that the dominant phonon scattering mechanism at low temperatures is due to acoustic phonons. At low temperatures only the emission process takes place, since there are not enough

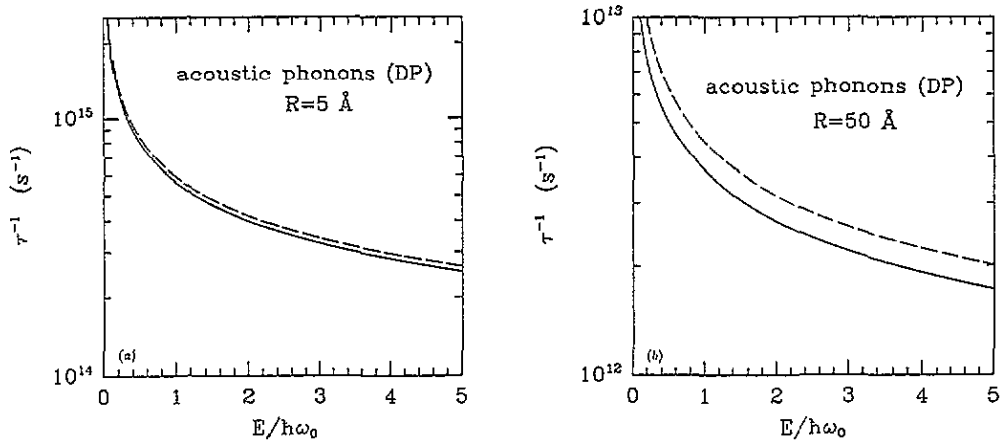

Figure 2. The inverse scattering time τ^{-1} due to the electron–acoustic-phonon interaction in the deformation potential coupling for the size quantum limit in a quantum-well wire of circular cross-section, (a) with radius $R = 50$ Å, and (b) with radius $R = 100$ Å. Full and broken curves give τ^{-1} with and without screening, respectively, for the emission process at $T = 300$ K.

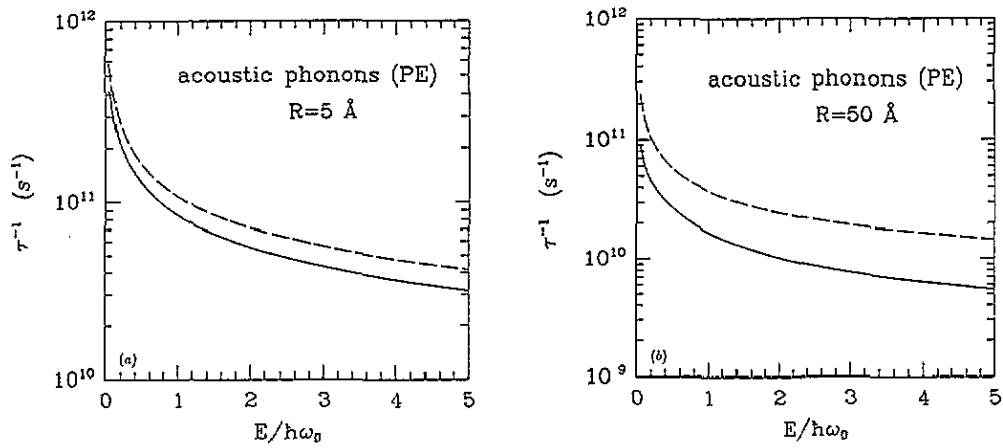

Figure 3. The inverse scattering time τ^{-1} due to the electron–acoustic-phonon interaction in the piezoelectric coupling for the size quantum limit in a quantum-well wire of circular cross-section, (a) with radius $R = 50$ Å, and (b) with radius $R = 100$ Å. Full and broken curves give τ^{-1} with and without screening, respectively, for the emission process at $T = 300$ K.

phonons to be absorbed. It is interesting to note that the scattering rates due to electron–optical-phonon and electron-deformation potential coupled acoustic phonon interactions are quite comparable, within an order of magnitude, at $T = 300$ K.

It has been argued [9, 17] that the dimensionality effects are enhanced in 1D structures, and the singularity in the phonon emission rate at $E = \hbar\omega_0$ (for the electron–optical-phonon interaction) is a consequence of the 1D density of states, which is proportional to $(E/\hbar\omega_0 \mp 1)^{-1/2}$ for emission and absorption processes,

respectively. That there is no phonon emission below $E = \hbar\omega_0$ (see figures 1(*a*) and (*b*)) comes from the fact that we assume the bulk optical phonons are dispersionless, namely $\omega_q = \omega_0$. Similar density of states effects occur for electron–acoustic-phonon emission rates (see figures 2(*a*)–3(*b*)), but because of the elastic approximation we employ, the onset of phonon emission is shifted to $E = 0$. To assess the validity of the elastic approximation ($E(k_z)$ or $E(k'_z) \gg \hbar\omega_q$), we have also performed the rate calculations for the electron–acoustic-phonon interaction without this assumption, finding no significant changes at the level of accuracy sought here.

In considering the effects of screening on the electron–phonon scattering rates in Q1D quantum-well wires, we have used the dielectric function $\varepsilon(q)$ in the RPA. For GaAs with carrier density $n = 1.3 \times 10^{17}\,\mathrm{cm}^{-3}$, and assuming the effective-mass of electrons to be $m = 0.07m_e$, we obtain $r_s = 15.7$. Although, strictly speaking, the RPA is valid only for $r_s \ll 1$ (the high-density limit), we have found that the scattering rates are not altered very much by using, for example, the Hubbard approximation to the dielectric function. In figure 4 we show the temperature-dependent static dielectric function $\varepsilon(q)$ at $T = 300\,\mathrm{K}$ (indicated by the full curve), in comparison to the zero-temperature $\varepsilon(q)$ (indicated by the broken curve) in the RPA. Evidently, the temperature dependence modifies $\varepsilon(q)$ at small q, which in turn is quite different than the non-interacting dielectric function in the same region. Examining the various forms of the electron–phonon interaction parameter $C(q)$ (7)–(9) and considering their contribution to the scattering time τ, we expect the effects of screened interactions to be largest for the electron–optical-phonon scattering and smallest for the electron–acoustic-phonon scattering (deformation potential). This is clearly seen in figures 1(*a*)–3(*b*). We have accounted for the temperature dependence of the dielectric function using the formulation [24] given in the previous section. This has been crucial [15] in softening the divergence at $q = 2k_F$ in the 1D dielectric function. In our case, since we use the 3D $\varepsilon(q)$ to screen the interaction of electrons with bulk phonons, a temperature-dependent $\varepsilon_T(q)$ is incorporated for consistency. Indeed, we have found that the temperature dependence of the dielectric function has an effect of lowering the scattering rates. It is clear from figure 4 that the screening effects would be more significant at low temperatures than high temperatures, as noticed by other researchers. As pointed out earlier, the model of the dielectric function we use is more appropriate to an unconfined system of electrons, since we have not evaluated $\varepsilon_T(q)$ using the wavefunctions given in (1). Within the RPA dielectric function employed here, this would possibly modify the small-q region of $\varepsilon(q)$ (and consequently $\varepsilon_T(q)$) as depicted in figure 4. We believe the qualitative results reached here will remain the same upon the inclusion of more sophisticated models of the dielectric function.

Constantinou and Ridley [17] have found ~25% reduction in the scattering rates due to the finite depth of the confining quantum-well in Q1D semiconductor structures. Our investigation shows a similar order-of-magnitude effect can be accounted for by screened electron–phonon interactions. Therefore, if screened electron–phonon interactions are used with a finite quantum-well model of confinement, further reduction in the scattering rates is possible. The lowering in the scattering rates due to screened electron–phonon interactions, made explicit in our calculations, have been previously anticipated [9, 25]. Although we have presented our results only for GaAs, with the appropriate choice of the material parameters different substances such as InAs, InSb, CdS, etc., can also be studied. Finally, we note that the relaxation time τ_t, and hence the mobility μ, can also be calculated using the screened electron–phonon

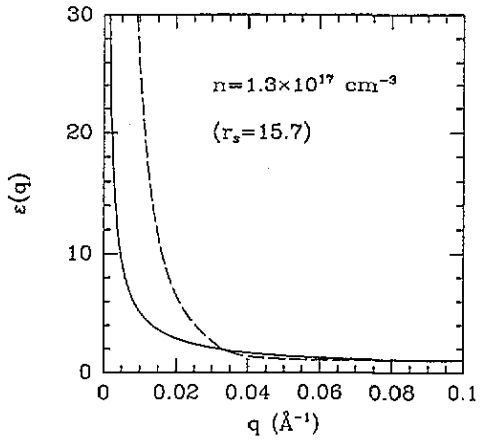

Figure 4. The temperature-dependent dielectric function used in the screened electron–phonon interactions. Full curve: $\varepsilon_T(q)$ at $T = 300$ K, broken curve: $\epsilon(q)$ at $T = 0$, both in the RPA.

interactions discussed here. The lowering of the scattering rates due to screened electron–phonon interactions will enhance the mobility in Q1D samples which will have important technological implications in terms of device applications.

4. Summary

We have studied the size effects on the screened electron–phonon interactions in Q1D quantum-well wires by calculating the scattering rates. We have considered the interaction of electrons with polar-optical and acoustic phonons. Acoustic phonons, in turn, are treated in the deformation potential and piezoelectric couplings. Screening effects are introduced by renormalizing the electron–phonon interactions with the temperature-dependent dielectric function $\varepsilon_T(q)$. Effects of screened electron–phonon interactions on the single-particle scattering rates are strongest in the case of electron–optical-phonon scattering. The scattering rates due to the electron–acoustic-phonon interaction in the deformation potential coupling are found to be comparable to the electron–optical-phonon interaction.

Acknowledgments

We acknowledge the support of TUBITAK under grant number TBAG-1155. We also thank Professor Abdus Salam and the Condensed Matter Group for their hospitality at the International Centre for Theoretical Physics, Trieste, where part of this work has been done. Fruitful discussions with Professors M Tomak and A Erçelebi are gratefully acknowledged.

References

[1] Sakaki H 1980 *Japan. J. Appl. Phys.* **19** L735

[2] Petroff P M, Gossard A C, Logan R A and Wiegmann W 1982 *Appl. Phys. Lett.* **41** 635
[3] Thornton T J, Pepper M, Ahmed H, Andrews D and Davies G J 1986 *Phys. Rev. Lett.* **56** 1198
[4] Cibert J, Petroff P M, Dolan G J, Pearton S J, Gossard A C and English J H 1986 *Appl. Phys. Lett.* **49** 1275
[5] Temkin H, Dolan G J, Parish M B and Chu S N G 1987 *Appl. Phys. Lett.* **40** 413
[6] Tonucci R C, Justus B L, Campillo A J and Ford C E 19992 *Science* **258** 783
[7] Arora V 1981 *Phys. Rev.* B **23** 5611; 1981 *Phys. Status Solidi* B **105** 707
[8] Riddock F A and Ridley B K 1982 *Surf. Sci.* **142** 260
[9] Leburton J P 1984 *J. Appl. Phys.* **56** 2850
[10] Briggs S and Leburton J P 1988 *Phys. Rev.* B **38** 8163
[11] Iafrate G J, Kerry D K and Reich R K 1982 *Surf. Sci.* **113** 485
[12] Briggs S, Mason B A and Leburton J P 1989 *Phys. Rev.* B **40** 12001
[13] Gold A and Ghazali A 1990 *Phys. Rev.* B **41** 7626
[14] Lee J and Spector H N 1983 *J. Appl. Phys.* **54** 3921
[15] Fishman G 1986 *Phys. Rev.* B **34** 2394; 1987 *Phys. Rev.* B **36** 7448
[16] Bastard G, Brum J A and Ferreira R 1991 *Solid State Phys.* **44** 229
[17] Constantinou N C and Ridley B K 1989 *J. Phys.: Condens. Matter* **1** 2283
[18] Jovanovic D, Briggs S and Leburton J P 1990 *Phys. Rev.* B **42** 11108
[19] Leburton J P and Jovanovic D 1992 *Semicond. Sci. Technol.* **7** B202
[20] Campos V B, Degani M H and Hipólito O 1991 *Solid State Commun.* **79** 473
[21] Basu P K and Nag B R 1981 *J. Phys. C: Solid State Phys.* **14** 1519
[22] Lee J and Vassell M O 1984 *J. Phys. C: Solid State Phys.* **17** 2525
[23] Lee J and Spector H N 1985 *J. Appl. Phys.* **57** 366
[24] Arista N R and Brandt W 1984 *Phys. Rev.* A **29** 1471
Maldague P 1978 *Surf. Sci.* **73** 296
[25] Shah J, Pinczuk A, Störmer H L, Gossard A C and Wiegmann W 1983 *Appl. Phys. Lett.* **42** 55